DeCarbon 10 (2025) 100137

Contents lists available at ScienceDirect

DeCarbon

journal homepage: www.sciencedirect.com/journal/decarbon

Research Article

Toward carbon-zero internet of things: Soil-powered renewable energy for perpetual sensing and communication

Yaozi Zheng[a,1], Yawei Wang[a,1], Jingyi Liu[a,b], Junlei Wang[c,*], Guobiao Hu[a,**]

[a] Thrust of Internet of Things, The Hong Kong University of Science and Technology (Guangzhou), Guangzhou, Guangdong 511400, China
[b] State Key Laboratory of Maritime Technology and Safety, Marine Engineering College, Dalian Maritime University, Dalian, China
[c] School of Mechanical and Power Engineering, Zhengzhou University, Zhengzhou 450001, China

ARTICLE INFO

Keywords:
Soil microbial fuel cell
Energy harvesting
Internet of things (IoT)
Low-power circuit
Renewable energy

ABSTRACT

The widespread deployment of Internet of Things (IoT) devices has led to an increasing demand for sustainable and cost-effective power resources. Soil microbial fuel cells (SMFCs) have emerged as a promising solution, offering great biocompatibility and operational viability. This study presents a thorough investigation of the critical design parameters that influence the performance of SMFCs, with a particular focus on electrode material selection and electrode spatial configurations. Six common metallic materials, including brass, copper, stainless steel, aluminum alloy, iron, and zinc, are evaluated for their effectiveness as electrode materials, with zinc-stainless steel being found to be the optimal combination based on voltage and current outputs. The spatial arrangement of the electrodes is also shown to impact performance, with the series connection mode providing higher voltage output and larger internal resistance, while the parallel mode results in higher power output and lower internal resistance. To showcase the practical potential of SMFCs, a nine-cell series array was utilized to power a customized low-power IoT node, enabling the successful transmission of temperature data to the cloud without the need for a traditional battery. This work highlights the viability of SMFCs as a renewable, battery-free solution for IoT devices, with potential applications in agriculture, environmental monitoring, and smart campuses.

1. Introduction

The need for frequent battery replacement in large-scale IoT system deployment increases maintenance costs and environmental burdens [1–5]. To address this issue, renewable energy sources such as solar and wind power have been explored [6,7]. However, solar energy highly relies on sunlight, making it unreliable in shaded or indoor environments, and wind power is limited to specific geographical locations with sufficient airflow, restricting its applicability [8,9]. Additionally, both solutions entail high installation and maintenance costs, which hinder their widespread deployment in distributed IoT systems [10,11]. Given these limitations, there is a pressing need for a reliable, low-cost, and environmentally friendly power source to foster the development of self-sustaining IoT node devices [12,13]. In this context, energy harvesting technologies such as piezoelectric [14], triboelectric [15], thermoelectric [16], electromagnetic [17], and bioenergy systems have been widely investigated for converting ambient mechanical, thermal, or chemical energy into electricity [11]. Among these, soil microbial fuel cells (SMFCs) represent a promising solution with unique advantages over the traditional ones [18]. They can continuously generate power outputs independent of illumination or weather conditions and, through microbial metabolism, produce no harmful pollutants, thereby offering a clean and sustainable energy solution (see Supplementary Table S2) [19,20]. Moreover, SMFCs are cost-effective and easy to deploy, making them ideal for large-scale, eco-friendly distributed IoT systems.

The concept of SMFCs first appeared in 1911 when scientists discovered that microbes in soil could generate electricity [21]. In 1931, Barnett Cohen indicated that microbial metabolism could produce electric currents via electron transfer [22]. However, for decades, research on SMFCs remained limited. With advancements in electrochemical technology and the growing demand for sustainable power sources in IoT applications, SMFCs have gained recognition as a promising potential energy solution [23]. To enhance their efficiency, previous studies have explored various anode materials, which play a

* Corresponding author.
** Corresponding author.
E-mail addresses: jlwang@zzu.edu.cn (J. Wang), guobiaohu@hkust-gz.edu.cn (G. Hu).
[1] These authors contribute equally to this paper.

https://doi.org/10.1016/j.decarb.2025.100137
Received 17 September 2025; Received in revised form 8 November 2025; Accepted 15 November 2025
Available online 21 November 2025

critical role in electron transfer [24]. However, despite significant progress, practical applications of SMFCs have been scarcely reported [25]. In addition to material selection, the physical placement of the anode has a substantial impact on microbial community structure and diversity, thereby influencing SMFC performance [26]. Studies have shown that factors such as the electrode material, biocompatibility, conductivity, and spacing can influence SMFC performance, yet their precise impacts remain unclear [19,27]. Since systematic research and experimental studies on optimizing SMFC design are limited, guidelines for improving SMFC efficiency are lacking. Hence, further investigation is needed to thoroughly explore the optimization of anode materials, electrode placement, and other parameters to improve the design of SMFCs and enhance their performance.

This study aims to tackle these challenges, focus on optimizing SMFCs, and then apply them to a practical IoT application. Based on electrochemical principles and the microbial fuel cell theory (Fig. 1(a)), the research begins by investigating the effects of electrode materials, spacing, and configuration on the output of SMFCs. Experiments are conducted under carefully controlled conditions, with specific soil volume, temperature, and humidity levels. A constant temperature and humidity incubator (HWS-250) is utilized to maintain stable environmental conditions. For electrical measurement and monitoring, an electrometer (Keithley 6514) and an oscilloscope (DHO 1072) are utilized. Furthermore, we designed an energy management circuit (EMU) to regulate and store the energy harvested by the SMFC. Additionally, we developed a low-power consumption IoT node with sensing and communication capabilities. By integrating these components, we successfully built a battery-free IoT node capable of perpetually sensing and transmitting the ambient temperature data to the IoT cloud. Overall, this research presents an innovative approach for supplying energy to empower IoT nodes for perpetual operation in scenarios such as sustainable campuses, smart agriculture, etc.

2. Results

2.1. Overview of mechanisms and structures

Fig. 1(a) presents the schematic diagram of the SMFC, which consists of two electrodes made from different materials: the anode is buried in an oxygen-deficient (anaerobic) soil layer, while the cathode is positioned in an oxygen-rich (aerobic) region [19,28,29]. The soil serves as a medium for proton transfer and provides organic substrates necessary for microbial activities. During microbial metabolism, the microbes in the soil release electrons and transfer them to the anode, which then flows through the external wire to the cathode, generating an electrical current [23,30]. At the same time, protons migrate through the soil to the cathode, where they react with oxygen to produce water, completing the electrochemical process. When acetate is used as the organic substrate at the anode, the overall reaction in the SMFC can be simplified as:

$$CH_3COO^- + 2\,O_2 \rightarrow CO_2 + HCO_3^- + H_2O$$

The whole process can be divided into two half-reactions, each occurring at the respective electrodes. The oxidation half-reaction at the anode is as follows:

$$CH_3COO^- + 3\,H_2O \rightarrow CO_2 + HCO_3^- + 8\,H^+ + 8\,e^-$$

The reduction half-reaction on the cathode can be described as:

$$2\,O_2 + 8\,H^+ + 8\,e^- \rightarrow 4\,H_2O$$

Fig. 1(b–c) shows the prepared soil container for prototyping SMFCs used for material selection and electrode distribution tests. Unlike chemical batteries, which are non-recyclable and cannot be self-recharged, SMFCs harvest electricity from everlasting microbial metabolism activity in the soil, thereby producing zero pollution and minimizing environmental impact [31,32]. It can be envisioned that such SMFCs could be deployed to establish battery-free, eco-friendly IoT nodes for monitoring applications in the agriculture industry, such as temperature, humidity, and air quality. Fig. 1(d) shows an application scenario under development on the campus of the Hong Kong University of Science and Technology (Guangzhou).

2.2. Electrode material selection

Electrode materials play a crucial role in affecting the performance of SMFCs. Identified critical factors include surface area, roughness, electrical conductivity, and biocompatibility [33]. An ideal electrode should provide a large surface area and high roughness to facilitate microbial attachment, exhibit excellent electrical conductivity for electron transfer, and possess good biocompatibility to avoid disrupting microbial

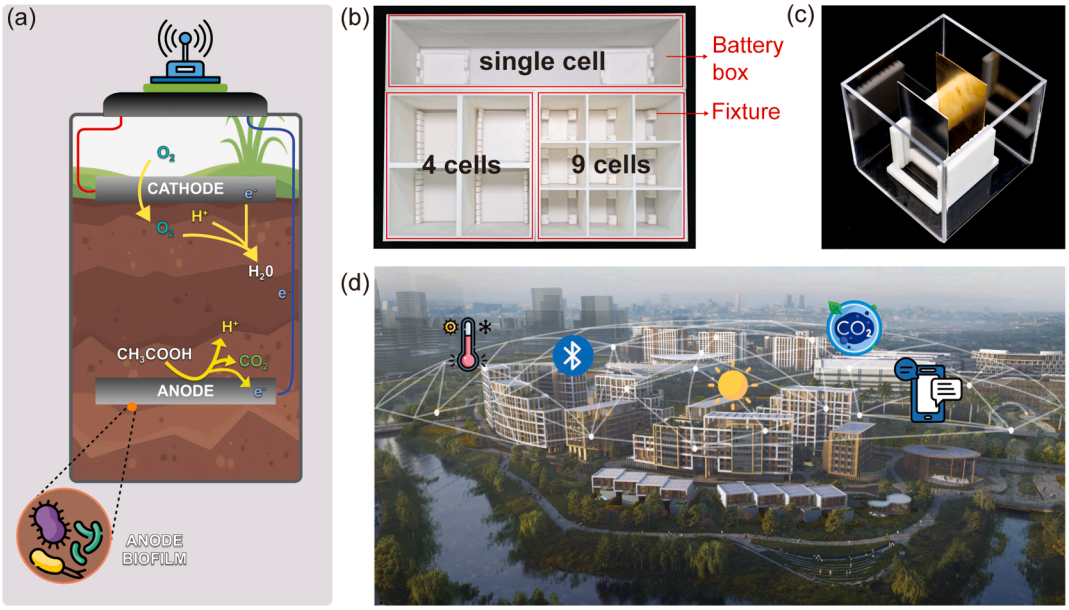

Fig. 1. (a) Working mechanism of the SMFC. (b–c) Soil containers prepared for SMFC prototyping. (d) Vision of sustainable, soil-powered distributed systems on campus.

activity [25]. However, there is limited research on SMFC electrode materials, and a quantitative evaluation of the influences of those factors is lacking. Metal materials, in particular, provide distinct advantages, such as superior electrical conductivity, enhanced mechanical durability, and ease of fabrication, making them well-suited for practical deployment in real-world SMFC applications [25]. In this study, six widely accessible metal materials, including brass, copper, stainless steel, aluminium alloy, iron, and zinc, are selected to assess their suitability as SMFC electrodes. The abbreviations for these materials are listed in Table I. To minimize the impact of external factors, the experiments are conducted in acrylic containers, each with dimensions of 10 cm × 10 cm × 10 cm in Fig. 1(c). The soil used in the experiment was unprocessed commercial potting soil, commonly used for flower cultivation and purchased in bulk to ensure a relatively homogeneous microbial and nutrient composition. Throughout the test, the soil was maintained in a moderately moist state, corresponding to the effective moisture range reported by Zhang et al. [34], who observed a sharp decline in SMFC's voltage output below a moisture content of 0.2, a steady increase between 0.2 and 0.4, and a plateau beyond 0.4. Accordingly, soil moisture was kept within the range of 50–60 %, while the ambient temperature and humidity were precisely controlled at 26 °C and 70 %, respectively, using a biochemical incubator. All the electrodes are cut to a fixed size, ensuring an identical contact area of 5 cm × 10 cm with the soil. The six electrodes were combined and grouped into 15 electrode pairs, with each pair individually inserted into the soil samples at an electrode spacing of 2.5 cm. For each electrode combination, ten independent samples were prepared to ensure statistical reliability. All SMFC samples were stabilized in an incubator for 36 h prior to testing and measurement, allowing sufficient microbial attachment and biofilm formation on the electrode surfaces.

As depicted in Fig. 2(a), among all samples, the brass-copper combination produces the lowest potential difference of only 0.015 V. Electrode pairs made of zinc with stainless steel, brass, or copper, as well as an aluminium-stainless steel combination, exhibit higher voltage of 0.81 V, 0.72 V, and 0.65 V, respectively. By comparing the results, a relative potential ranking of the six materials is established as follows: stainless steel > copper > brass > iron > aluminium > zinc. To examine voltage and current outputs, a three-day continuous test is conducted using the three highest-performing electrode pairs: zinc-stainless steel, zinc-copper, and stainless steel-aluminium, as demonstrated in Fig. 2(d). The current values represent instantaneous peak currents measured under short-circuit conditions using a Keithley 6514 electrometer, corresponding to the maximum steady-state output immediately after voltage stabilization. The results in Fig. 2(b) and (c) demonstrate that the zinc-stainless steel combination yields the highest performance, with an average open-circuit voltage of 0.87 V and a short-circuit current of 2.68 mA. Therefore, the electrode pair consisting of zinc (anode) and stainless steel (cathode) is identified as the optimal combination and chosen for further exploration in the following study. The observed performance hierarchy among different electrode pairs can be attributed to the interplay of intrinsic material properties, such as surface roughness, electrical conductivity, and biocompatibility. Surface roughness influences microbial attachment and biofilm formation, while conductivity governs the efficiency of electron transport. Biocompatibility modulates microbial metabolism and community stability. Among all the tested configurations, the zinc–stainless steel pair delivered the highest output, representing an optimal synergy between these physicochemical and biological factors that collectively enhance the SMFC's performance. To further interpret this result, scanning electron microscopy (SEM) images were captured for the post-use electrodes, as shown in Fig. 2(g). Compared with the SEM images of the unused electrodes, clear microbial adhesion and biofilm formation can be observed on the surfaces of both used electrodes, with a notably denser and more extensive biofilm coverage on the zinc anode. These morphological observations offer additional evidence supporting the microbial-driven electricity generation mechanism in SMFCs, and the superior biofilm development on zinc offers a plausible explanation for its enhanced performance as the anode. Moreover, both the anode and cathode surfaces remained intact, with no visible signs of corrosion or chemical degradation. The internal resistance exhibited minimal variation over the seven days, indicating stable and consistent operational performance. Short-term evaluations of the other electrode materials revealed similar trends in microbial attachment and electrical outputs, suggesting that the observed stability is broadly representative across all tested configurations.

Table 1
Abbreviations for selected metallic materials.

Metal Material	Abbreviation
Brass	Br
Copper	Cu
Iron	Fe
Stainless steel	SS
Aluminium	Al
Zinc	Zn

The spatial arrangement of electrodes, including their orientation and spacing, is another critical factor affecting the performance of SMFCs [34]. Previous studies have indicated that at a constant substrate feeding interval, smaller electrode spacings yield better performance at the beginning [35]. However, at the end of their long-term test, the conclusion was overturned, revealing that a larger electrode spacing showed the best performance. As external factors fluctuate over time and the increased discrepancies between different samples could distort the results [35], a short-term test is carried out to minimize these fluctuations and reduce their impact. As illustrated in Fig. 2(e)–a 0.001 m^3 container is divided into four equal sections, each fitted with zinc-stainless steel electrode pairs, all having an identical contact area of 4.5 cm × 10 cm. But their electrode spacings are set to 1 cm, 2 cm, 3 cm, and 4 cm, respectively. They are preserved under consistent environmental conditions for 7 days. The open-circuit voltage output and impedance matching results are presented in Fig. 2(f). The measurement platform and the detailed impedance matching curves used to calculate these power values are shown in Fig. S1. Each power point in Fig. 2(f) was derived from the impedance matching curves in Fig. S1. The experimental results indicate stable performance, characterized by an open-circuit voltage of 1 ± 0.02 V, an internal resistance of 500Ω and 600Ω, and a peak power of 0.1 ± 0.035 mW. It is important to note that power measurement in this test is challenging. Since shunting the SMFC to a resistive load dissipates energy instantly, with the dissipation rate varying with each instance, the voltage fluctuates when changing the resistances during the test.

Additionally, in the impedance matching test, resistance values are sampled at intervals of 100 Ω, which implies that a slight change in resistance may greatly change the calculated power. This explains why, although the variation in open-circuit voltage is negligible, the variation in power output is relatively noticeable. Based on the open-circuit voltage result and considering unavoidable measurement errors, these findings suggest that the electrode spacing has a limited impact on the performance of SMFCs in the short-term test under controlled conditions. The slight variations in the output might arise from many external factors, such as discrepancies in the soil composition and fluctuations of environmental conditions, rather than the inherent electrochemical properties of SMFCs. To complement the short-term performance evaluation, a 30-day open-circuit voltage monitoring experiment was conducted under indoor conditions using SMFCs with electrode spacings of 1, 2, 3, and 4 cm. As shown in Fig. 2(h), the voltage in all configurations slightly increased over time in the absence of external loads, but overall stabilizing within the range of 1.0–1.1 V. No substantial differences were observed among the different configurations, which is consistent with the short-term results and suggests that, within this range, electrode spacing has minimal influence on output voltage stability.

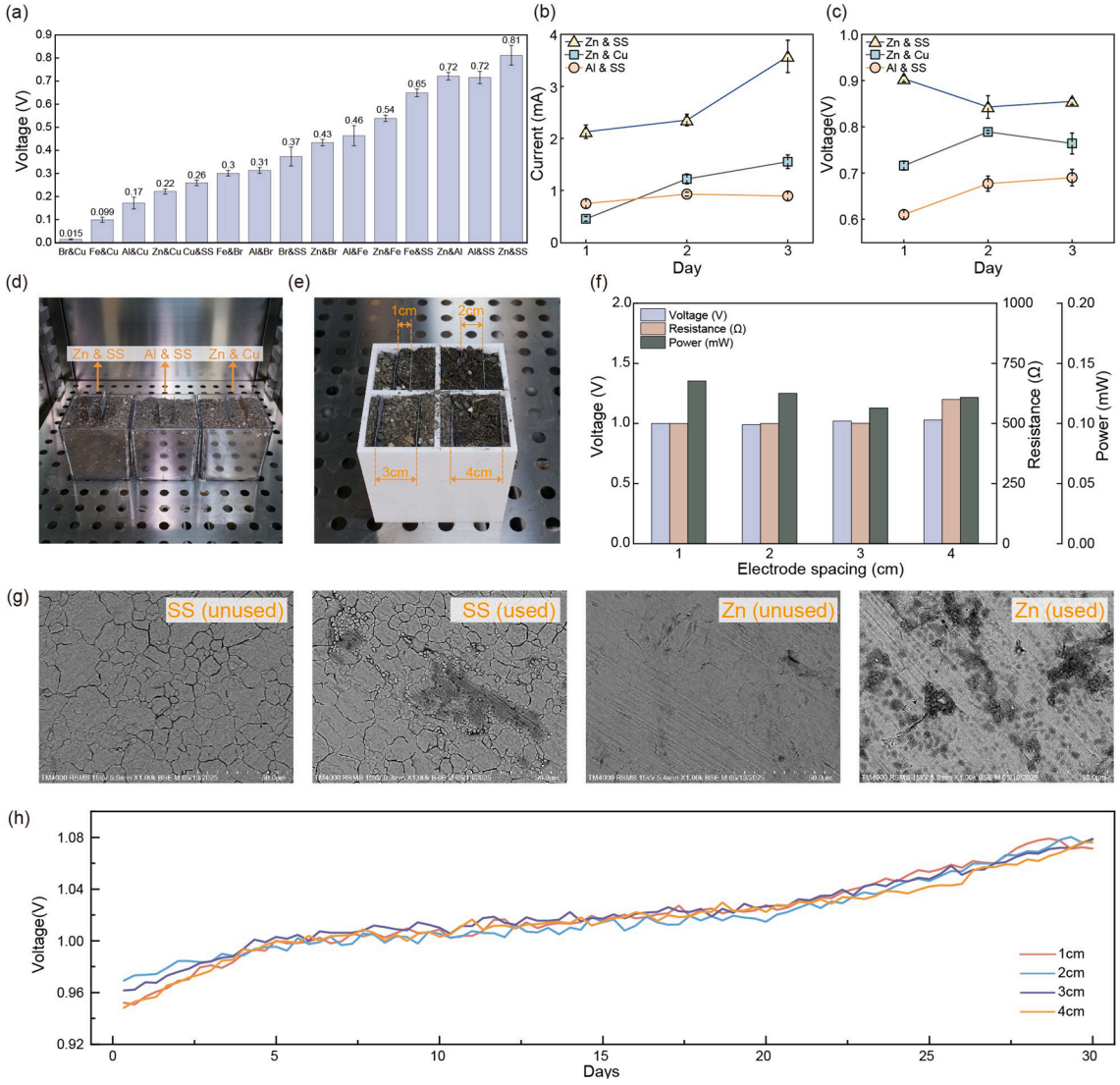

Fig. 2. Output performance of the SMFCs with various electrode materials and spacing. (a) Voltage outputs of the SMFCs with different electrode material combinations. (b) Instantaneous peak current and (c) Voltage outputs of the SMFCs with zinc-stainless steel, zinc-copper, and stainless steel-aluminium electrode material combinations over three days. (d) Experimental setups for electrode material selection. (e) Setup for electrode spacing tests. (f) Output performance of the SMFC using the zinc-stainless steel combination with different electrode spacings. (g) SEM images of stainless steel and zinc electrodes before and after 7 days of SMFC operation. (h) Voltage output of the SMFCs with different electrode spacings over a 30-day period.

2.3. Electrode spatial distribution experiment

To investigate the effect of electrode spatial distribution on the output performance of SMFCs, three containers are designed and fabricated, as shown in Fig. 1(b). They maintain the same total volume while being divided into a single cell, four cells, and nine cells. The electrodes are made of zinc and stainless steel, with a consistent surface area of 18 $cm^3$and an electrode spacing of 2 cm. After setting up the electrodes and filling the containers with soil, they were incubated under controlled conditions at 26 °C and 70 % humidity for three days. Over the following seven days, open-circuit voltage and current outputs were recorded ten times each day for all configurations, including single-cell, four-cell, and nine-cell SMFCs. For the SMFCs with four-cell and nine-cell configurations, repeated measurements were conducted under both series and parallel connection modes, resulting in five experimental groups.

Fig. 3(a–e) present the short-circuit current measurements recorded over seven days for the five experimental groups, and Fig. 3(f) offers a statistical analysis of these results. The parallel configurations exhibited superior current generation capabilities, with both the four-cell and nine-cell SMFCs exceeding 15 mA, outperforming the single-cell SMFC's output of 13 mA. In contrast, series-connected configurations demonstrated substantially reduced current outputs, with the nine-cell and four-cell series configurations generating 1.45 mA and 3.58 mA, respectively. Fig. 3(g) illustrates the voltage output characteristics of the five experimental groups. The nine-cell series configuration generated superior voltage output, with an open-circuit voltage of about 5.015 V, followed by the four-cell series configuration with a voltage output of approximately 2.737 V. In comparison, the single-cell SMFC and the four-cell and nine-cell parallel SMFCs exhibited significantly lower open-circuit voltage outputs, all below 1 V during the testing period.We additionally performed supplementary measurements on extended SMFC connection configurations, including a hybrid series–parallel arrangement. As summarized in Table S1, the hybrid configuration exhibited intermediate voltage and current outputs compared with the cases where the SMFCs were connected purely in series or purely in parallel, consistent with the performance trends predicted by circuit theory.

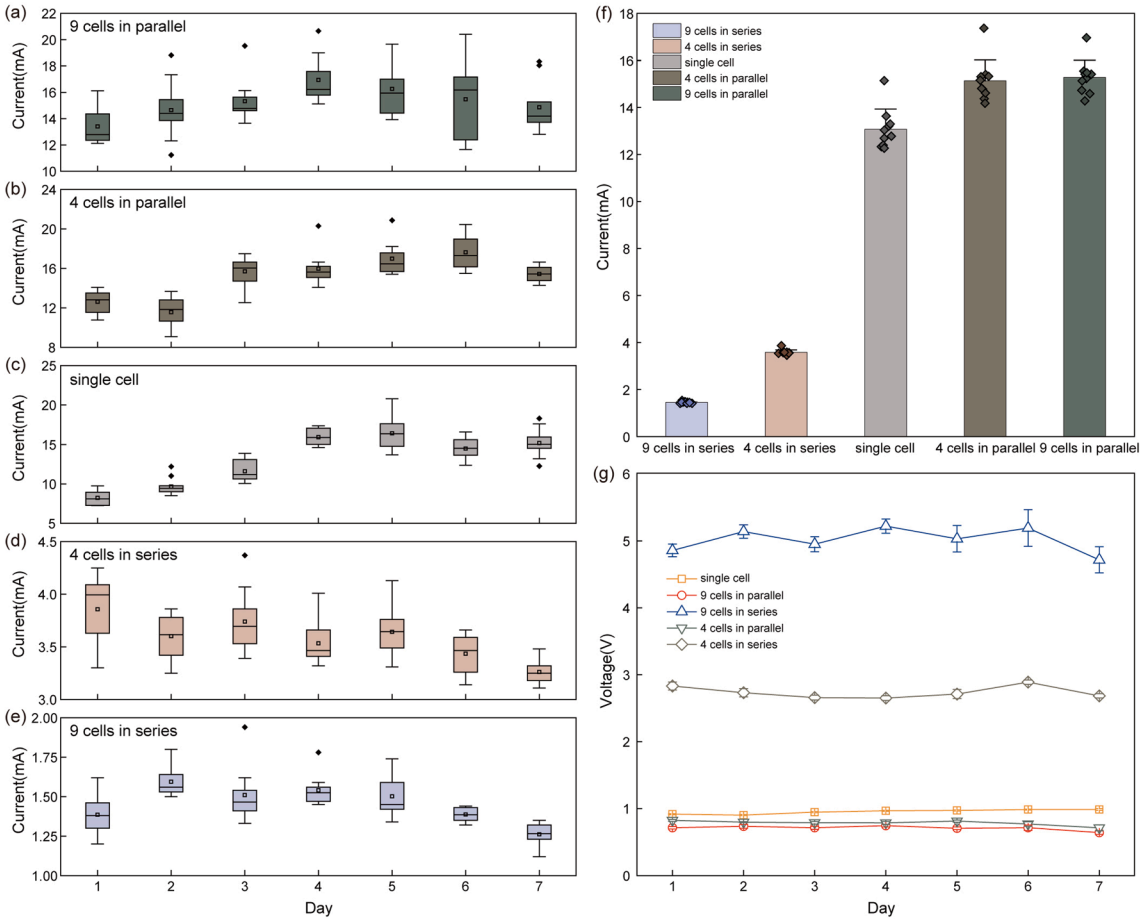

Fig. 3. Current (a–f) and voltage (g) outputs of SMFCs with different electrode spatial arrangements.

To ensure the reproducibility and statistical reliability of the experimental results, the dataset was expanded and quantitatively analyzed. During the seven-day test, five independent SMFC samples were prepared for voltage measurements, and another five samples for current measurements. Each sample was tested under the identical environmental conditions for seven consecutive days, with ten repeated measurements performed daily to assess stability and day-to-day variation. The compiled data were analyzed using one-way ANOVA, and the detailed statistics are summarized in Table S3, including the mean values, standard deviations, and corresponding p-values. The analysis revealed significant differences in both the voltage and current ($p = 7.82 \times 10^{-33}$ and $p = 9.81 \times 10^{-17}$, respectively), confirming the strong statistical significance and high reproducibility of the experimental results.

Impedance matching experiments further reveal differences in maximum power output across the configurations. As shown in Fig. 4,

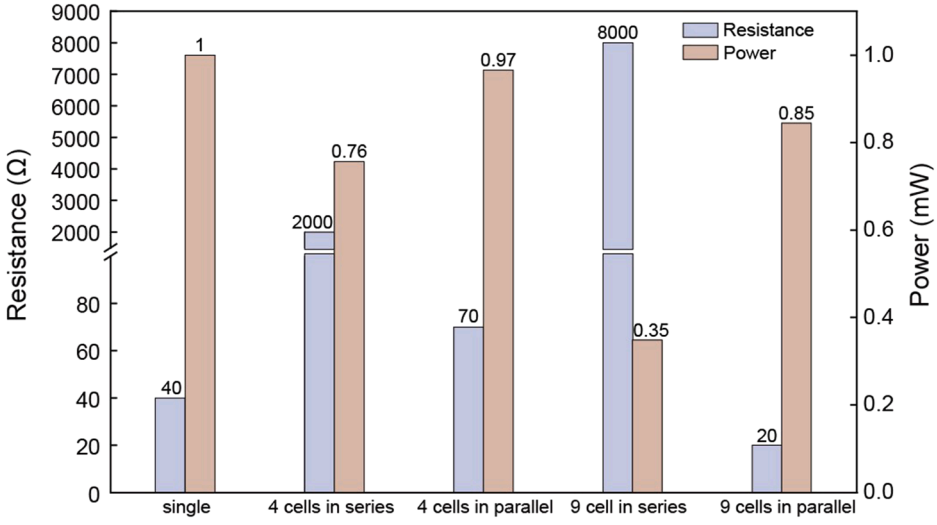

Fig. 4. Output performance of the SMFCs with different configurations and connection modes.

the single-cell exhibited the highest maximum power output of 1.00 mW, followed by the four-cell and nine-cell parallel configurations, which produced about 0.97 mW and 0.85 mW, respectively. The series configurations of the four-cell and nine-cell SMFCs generated the lowest power outputs of about 0.76 mW and 0.35 mW, respectively. The internal resistance of the nine-cell series SMFC is the highest, measuring 8000 Ω, followed by the four-cell series one with an internal resistance of about 2000 Ω. In contrast, the internal resistances of the single-cell SMFC and two parallel SMFCs are all below 80 Ω. This observed difference may primarily arise from the electrode area distribution: with the total electrode area maintained constant across configurations, each cell in multi-cell arrays has a smaller electrode area, resulting in higher internal resistance and lower per-cell power output [36]. Moreover, spatial variations in soil moisture, ion concentration, and microbial density in the array configuration can cause voltage imbalance, amplifying the performance gap [37,38]. Experimental results indicate that the electrode arrangement has a significant impact on the performance of SMFCs, including voltage and current outputs, as well as internal impedance. Hence, one knows that adjusting the spatial distribution of SMFCs and selecting appropriate connection modes can change voltage and current outputs to meet different load requirements. In addition, the single-cell SMFC developed in our study, using stainless steel and zinc as electrodes, achieved a power density of 555.6 mW/m^2 under impedance-matching conditions. This value is significantly higher than the 17.4 mW/m^2 reported by Yen et al. [19] using carbon-felt electrodes under comparable soil conditions. While differences in the soil composition and environmental factors limit the precision of direct comparisons, the substantial performance gap underscores the effectiveness of metal electrodes.

2.4. Application demonstration

In recent years, SMFC technology has been studied and explored as a potential power solution, with researchers attempting to showcase its application value [39]. However, because SMFCs typically deliver low power output, most studies cannot implement them in real-world applications to really address power supply issues [18]. Existing research on SMFCs primarily focuses on optimizing configurations to enhance power output, with few successful practical applications. In this study, to offer a deeper understanding of the value and potential of this technique, we have carefully designed and prepared a practical application demonstration. Considering most electronic devices operate within a voltage range of 3.3 V–5 V, we use a nine-cell series SMFC to power the device in the following study.

As depicted in Fig. 5(c), the SMFC-powered IoT node consists of a nine-series SMFC and a customized low-power IoT node that can conduct sensing and communication. The working schematic of this IoT node is illustrated in Fig. 5(e). The power generated by the SMFC is

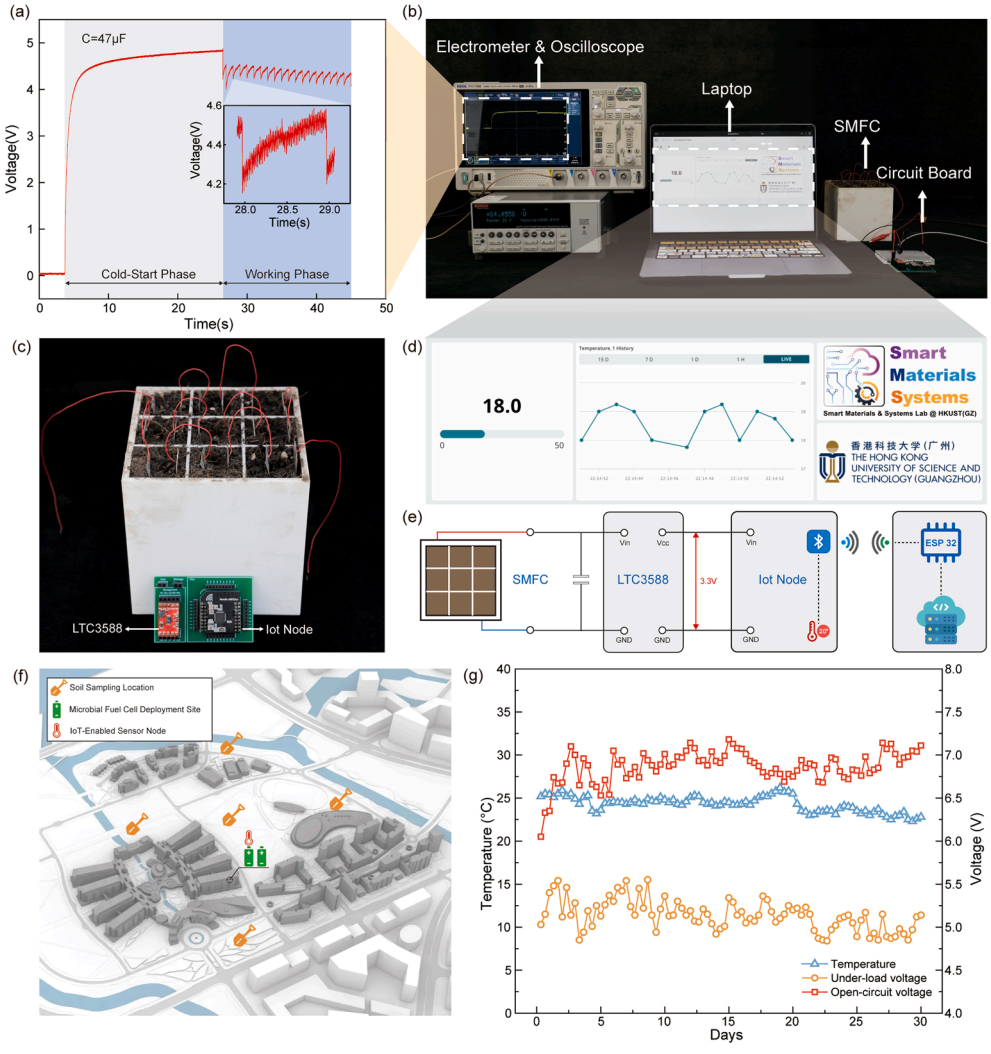

Fig. 5. (a) Voltage history of the capacitor during the operation process of the SMFC-powered IoT node. (b) Physical layout of the testing platform. (c) Nine-cell series SMFC connected to the low-power IoT node. (d) Temperature data uploaded to the cloud and displayed on the laptop. (e) The integrated system architecture, illustrating the flow of harvested energy through a 47 μF energy storage capacitor, the LTC3588 energy management chip, and the IoT node. (Multimedia – Video S1 available online). (f) Schematic map of the demonstration experiment showing the five campus soil sampling locations and the deployment site of the SMFC used to power the IoT sensor. (g) Temperature data collected by the SMFC-powered sensor over a 30-day period, along with the open-circuit voltage histories of both the active SMFC (driving the sensor) and the idle SMFC (under open-circuit conditions).

stored in a 47 μF capacitor, which cooperates with the LTC3588 chip for energy management. When the capacitor voltage is charged over 4.9V, which is the Undervoltage lockout threshold (UVLO) of the LTC3588, the chip provides a stabilized 3.3V output to the IoT device. The embedded chip of the IoT node includes a built-in temperature sensor, and it transmits the data via Bluetooth to a receiver built on an ESP32 microcontroller, which then uploads the data to the IoT cloud. The real-time operating interface of this SMFC-powered IoT system is shown in Fig. 5(d).The platform shown in Fig. 5(b) is designed to assess the performance of SMFCs and the connected IoT nodes they power. It enables the evaluation of SMFC energy output and the operational efficiency of IoT nodes, focusing on power stability, energy consumption, and data transmission reliability. It includes an electrometer and an oscilloscope for measurements, a laptop for displaying sensing data, and an SMFC-powered IoT node.

Fig. 5(a) shows the voltage charging history during the operation of the IoT node. During the cold-start phase, the voltage across the storage capacitor increases from 0 V to 4.9 V within approximately 23 s. Once the voltage reaches 4.9 V, the LTC3588 power management circuit begins to supply continuous, regulated power to the node and ceases output when the voltage drops to approximately 3.5 V, allowing recharging. Under steady-state operation, the node transmits 12 bytes of temperature data every second at a radio output power of 0 dBm. Within the 4.9–3.5 V operating range, the 47 μF capacitor provides approximately 276 μJ of useable energy. The first transmission after a cold start consumes about 125 μJ, while subsequent cycles stabilize at around 82 μJ. Even under extreme conditions where the SMFC output current is insufficient to promptly replenish the capacitor, the stored energy can sustain at least two complete transmission events, ensuring robust and continuous operation. A demonstration of using the SMFC to supply the IoT node is available in Video S1. This demonstration showcases the feasibility and reliability of using the SMFCs for practical IoT applications. To further evaluate environmental robustness, an additional experiment was conducted using unprocessed soil randomly collected from five locations across our university campus. As shown in Fig. 5(f), two SMFCs were constructed: one was used to power an IoT node for 1 h per day, while the other remained idle. For both SMFCs, voltage was measured three times daily throughout the experiment. The soil was left in its natural state without any pretreatment and maintained under identical indoor environmental conditions for both SMFCs. As presented in Fig. 5(g), the SMFC-powered sensor performed stably, and the voltage outputs of both the active and idle SMFCs remained within a consistent range over the 30-day period. These results demonstrate that SMFCs can reliably operate using naturally variable soil, reinforcing their feasibility for powering IoT devices outside of tightly controlled laboratory environments. In addition, visual inspection after the 30-day test revealed no noticeable electrode corrosion or structural deterioration, confirming the good electrode integrity, stable microbial activity, and consistent electrochemical performance throughout prolonged operation.Consistent with these observations, a broader comparison with previous SMFC systems (Table S4) shows enhanced power stability and sustained operation. The integration with a continuously operating wireless IoT node highlights a clear application-level innovation with improved practicality.

Supplementary video related to this article can be found at https://doi.org/10.1016/j.decarb.2025.100137

3. Conclusion

This study has thoroughly examined the electrochemical potential of widely accessible metal electrodes in soil and identified zinc and stainless steel as the most effective electrode pair for SMFCs. The influence of electrode spatial configuration on SMFC performance has also been comprehensively investigated. The results revealed that while the in-series connection mode increases the voltage output and the in-parallel connection mode enhances the current output, neither configuration significantly improves the overall energy conversion efficiency of SMFCs. However, adjusting the electrode arrangement could alter the output characteristics of SMFCs, providing a way to tailor the system for specific energy demands. To demonstrate the potential value of SMFCs in practical applications, an SMFC-powered IoT node was developed and used to power a customized low-power IoT node. An energy management circuit was employed to regulate energy collection and consumption. The demonstration showed that the system can self-sustain and operate using energy harvested by the SMFC from 0.001 m^3 of soil. Moreover, the system maintained continuous temperature monitoring and data transmission during the test, demonstrating its potential as a stable, low-maintenance power solution. In general, this study advances the development of SMFCs for self-powered IoT applications by optimizing electrode selection and spatial configuration, as well as designing customized low-power circuits. The effective deployment of the SMFC-powered IoT node has demonstrated its feasibility and value, laying the foundation for future improvements in efficiency and scalability, ultimately contributing to the advancement of sustainable energy solutions.

CRediT authorship contribution statement

Yaozi Zheng: Writing – original draft, Visualization, Validation, Software, Methodology, Investigation, Formal analysis, Data curation. **Yawei Wang:** Writing – original draft, Visualization, Validation, Software, Methodology, Investigation, Formal analysis, Data curation. **Jingyi Liu:** Methodology, Investigation, Formal analysis, Data curation. **Junlei Wang:** Writing – review & editing, Supervision, Project administration, Investigation. **Guobiao Hu:** Writing – review & editing, Supervision, Resources, Project administration, Methodology, Investigation, Funding acquisition, Conceptualization.

Declaration of interests

The authors declare that they have no known competing financial interests or personal relationships that could have appeared to influence the work reported in this paper.

Acknowledgment

This work was financially supported by the National Natural Science Foundation of China (Grant No. 52305135), the Guangzhou Municipal Science and Technology Bureau (Grant Nos. SL2023A03J00869, SL2023A04J01741), the Guangdong Provincial Key Lab of Integrated Communication, Sensing and Computation for Ubiquitous Internet of Things (Grant No. 2023B1212010007), the Guangzhou Municipal Science and Technology Project (Grant No. 2023A03J0011), and the Guangzhou Municipal Key Laboratory on Future Networked Systems (Grant No. 024A03J0623).

Appendix A. Supplementary data

Supplementary data to this article can be found online at https://doi.org/10.1016/j.decarb.2025.100137.

References

[1] H. Jayakumar, K. Lee, W.S. Lee, A. Raha, Y. Kim, V. Raghunathan, Powering the internet of things, in: Proc. 2014 Int. Symp. Low Power Electron. Des., ACM, La Jolla California USA, 2014, pp. 375–380, https://doi.org/10.1145/2627369.2631644.

[2] W. Mrozik, M. Ali Rajaeifar, O. Heidrich, P. Christensen, Environmental impacts, pollution sources and pathways of spent lithium-ion batteries, Energy Environ. Sci. 14 (2021) 6099–6121, https://doi.org/10.1039/D1EE00691F.

[3] Y. Li, X. Peng, Y. Li, D. Li, G. Hu, Catapult mechanism-enabled push-button energy harvester designed for capturing ultra-low frequency motion, Mech. Syst. Signal Process. 225 (2025) 112268, https://doi.org/10.1016/j.ymssp.2024.112268.

[4] Y. Wang, H. Du, H. Yang, Z. Xi, C. Zhao, Z. Qian, X. Chuai, X. Peng, H. Yu, Y. Zhang, X. Li, G. Hu, H. Wang, M. Xu, A rolling-mode triboelectric nanogenerator with multi-tunnel grating electrodes and opposite-charge-enhancement for wave energy harvesting, Nat. Commun. 15 (2024) 6834, https://doi.org/10.1038/s41467-024-51245-5.
[5] Q. Zhao, K. Sun, X. Wang, Q. Wang, J. Wang, Examining green-sustainable approaches for recycling of lithium-ion batteries, DeCarbon 3 (2024) 100034, https://doi.org/10.1016/j.decarb.2023.100034.
[6] Z. Şen, Solar energy in progress and future research trends, Prog. Energy Combust. Sci. 30 (2004) 367–416, https://doi.org/10.1016/j.pecs.2004.02.004.
[7] F. Blaabjerg, K. Ma, Wind energy systems, Proc. IEEE 105 (2017) 2116–2131, https://doi.org/10.1109/JPROC.2017.2695485.
[8] N. Kannan, D. Vakeesan, Solar energy for future world: - a review, Renew. Sustain. Energy Rev. 62 (2016) 1092–1105, https://doi.org/10.1016/j.rser.2016.05.022.
[9] G.M. Joselin Herbert, S. Iniyan, E. Sreevalsan, S. Rajapandian, A review of wind energy technologies, Renew. Sustain. Energy Rev. 11 (2007) 1117–1145, https://doi.org/10.1016/j.rser.2005.08.004.
[10] N.Q. Mohammed, M.S. Ahmed, M.A. Mohammed, O.A. Hammood, H.A.N. Alshara, A.A. Kamil, Comparative analysis between solar and wind turbine energy sources in IoT based on economical and efficiency considerations, in: 2019 22nd Int. Conf. Control Syst. Comput. Sci. CSCS, 2019, pp. 448–452, https://doi.org/10.1109/CSCS.2019.00082.
[11] V.D. Paccoia, F. Bonacci, G. Clementi, F. Cottone, I. Neri, M. Mattarelli, Toward field deployment: tackling the energy challenge in environmental sensors, Sensors 25 (2025) 5618, https://doi.org/10.3390/s25185618.
[12] FarisA. Almalki, S.H. Alsamhi, R. Sahal, J. Hassan, A. Hawbani, N.S. Rajput, A. Saif, J. Morgan, J. Breslin, Green IoT for eco-friendly and sustainable smart cities: future directions and opportunities, Mobile Network. Appl. 28 (2023) 178–202, https://doi.org/10.1007/s11036-021-01790-w.
[13] M. Shirvanimoghaddam, K. Shirvanimoghaddam, M.M. Abolhasani, M. Farhangi, V. Zahiri Barsari, H. Liu, M. Dohler, M. Naebe, Towards a green and self-powered internet of things using piezoelectric energy harvesting, IEEE Access 7 (2019) 94533–94556, https://doi.org/10.1109/ACCESS.2019.2928523.
[14] Y. Zhang, Y. Wang, J. Wang, G. Hu, Modeling and Analysis of VIV-galloping Coupled Piezoelectric Energy Harvester Shunted to SECE Interface Circuit, IEEEASME Trans. Mechatron., 2025, pp. 1–12, https://doi.org/10.1109/TMECH.2025.3603589.
[15] S. Liu, S. Liao, D. Liu, W. Qing, K. Wei, L. Zhao, H. Zou, A compact hybridized triboelectric-electromagnetic road energy harvester for vehicle speed measurement, DeCarbon 3 (2024) 100036, https://doi.org/10.1016/j.decarb.2024.100036.
[16] Q. Le, H. Cheng, J. Ouyang, Flexible combinatorial ionic/electronic thermoelectric converters to efficiently harvest heat from both temperature gradient and temperature fluctuation, DeCarbon 1 (2023) 100003, https://doi.org/10.1016/j.decarb.2023.100003.
[17] Y. Li, Y. Li, Y. Wang, M. Xiao, H. Tang, Y. Zi, J. Wang, X. Li, W.-H. Liao, G. Hu, From nature's deadly strike to safety protection: mantis shrimp-inspired ultrafast energy transformation for smart surveillance, Device 0 (2025), https://doi.org/10.1016/j.device.2025.100903.
[18] S.Z. Abbas, J.-Y. Wang, H. Wang, J.-X. Wang, Y.-T. Wang, Y.-C. Yong, Recent advances in soil microbial fuel cells based self-powered biosensor, Chemosphere 303 (2022) 135036, https://doi.org/10.1016/j.chemosphere.2022.135036.
[19] B. Yen, L. Jaliff, L. Gutierrez, P. Sahinidis, S. Bernstein, J. Madden, S. Taylor, C. Josephson, P. Pannuto, W. Shuai, G. Wells, N. Arora, J. Hester, Soil-powered computing: the engineer's guide to practical soil microbial fuel cell design, Proc. ACM Interact. Mob. Wearable Ubiquitous Technol. 7 (2023) 1–40, https://doi.org/10.1145/3631410.
[20] F. Sun, J. Chen, M. Tang, Y. Yang, Recent research progress, challenges and future directions of sediment microbial fuel cell: a comprehensive review, Int. J. Hydrogen Energy 50 (2024) 870–886, https://doi.org/10.1016/j.ijhydene.2023.09.112.
[21] M.C. Potter, Electrical effects accompanying the decomposition of organic compounds, Proc. R. Soc. Lond. - Ser. B Contain. Pap. a Biol. Character 84 (1911) 260–276.
[22] B. Cohen, The bacterial culture as an electrical half-cell, J. Bacteriol. 21 (1931) 18–19.
[23] T. Cai, L. Meng, G. Chen, Y. Xi, N. Jiang, J. Song, S. Zheng, Y. Liu, G. Zhen, M. Huang, Application of advanced anodes in microbial fuel cells for power generation: a review, Chemosphere 248 (2020) 125985, https://doi.org/10.1016/j.chemosphere.2020.125985.
[24] A. Rinaldi, B. Mecheri, V. Garavaglia, S. Licoccia, P. Di Nardo, E. Traversa, Engineering materials and biology to boost performance of microbial fuel cells: a critical review, Energy Environ. Sci. 1 (2008) 417, https://doi.org/10.1039/b806498a.
[25] S.Z. Abbas, Y.-C. Yong, F.-X. Chang, Anode materials for soil microbial fuel cells: recent advances and future perspectives, Int. J. Energy Res. 46 (2022) 712–725, https://doi.org/10.1002/er.7288.
[26] Y. Wu, H. Wu, H. Fu, Z. Dai, Z. Wang, Burial depth of anode affected the bacterial community structure of sediment microbial fuel cells, Environ. Eng. Res. 25 (2020) 871–877, https://doi.org/10.4491/eer.2019.362.
[27] J. Wang, H. Deng, S.-S. Wu, Y.-C. Deng, L. Liu, C. Han, Y.-B. Jiang, W.-H. Zhong, Assessment of abundance and diversity of exoelectrogenic bacteria in soil under different land use types, Catena 172 (2019) 572–580, https://doi.org/10.1016/j.catena.2018.09.028.
[28] C. Santoro, C. Arbizzani, B. Erable, I. Ieropoulos, Microbial fuel cells: from fundamentals to applications. A review, J. Power Sources 356 (2017) 225–244, https://doi.org/10.1016/j.jpowsour.2017.03.109.
[29] R.M. Allen, H.P. Bennetto, Microbial fuel-cells: electricity production from carbohydrates, Appl. Biochem. Biotechnol. 39–40 (1993) 27–40, https://doi.org/10.1007/BF02918975.
[30] H. Deng, Y.-C. Wu, F. Zhang, Z.-C. Huang, Z. Chen, H.-J. Xu, F. Zhao, Factors affecting the performance of single-chamber soil microbial fuel cells for power generation, Pedosphere 24 (2014) 330–338, https://doi.org/10.1016/S1002-0160(14)60019-9.
[31] S.Z. Abbas, M. Rafatullah, Recent advances in soil microbial fuel cells for soil contaminants remediation, Chemosphere 272 (2021) 129691, https://doi.org/10.1016/j.chemosphere.2021.129691.
[32] C. Abourached, T. Catal, H. Liu, Efficacy of single-chamber microbial fuel cells for removal of cadmium and zinc with simultaneous electricity production, Water Res. 51 (2014) 228–233, https://doi.org/10.1016/j.watres.2013.10.062.
[33] H.-C. Chang, W. Gustave, Z.-F. Yuan, Y. Xiao, Z. Chen, One-step fabrication of binder-free air cathode for microbial fuel cells by using balsa wood biochar, Environ. Technol. Innov. 18 (2020) 100615, https://doi.org/10.1016/j.eti.2020.100615.
[34] D. Zhang, Y. Ge, W. Wang, Study of a terrestrial microbial fuel cell and the effects of its power generation performance by environmental factors, in: Proc. 2013 Int. Conf. Adv. Mechatron. Syst., 2013, pp. 445–448, https://doi.org/10.1109/ICAMechS.2013.6681825.
[35] I.M. Simeon, A. Weig, R. Freitag, Optimization of soil microbial fuel cell for sustainable bio-electricity production: combined effects of electrode material, electrode spacing, and substrate feeding frequency on power generation and microbial community diversity, Biotechnol. Biofuels Bioprod. 15 (2022) 124, https://doi.org/10.1186/s13068-022-02224-9.
[36] S.-W. Im, H.-J. Lee, J.-W. Chung, Y.-T. Ahn, The effect of electrode spacing and size on the performance of soil microbial fuel cells (SMFC), J. Korean Soc. Environ. Eng. 36 (2014) 758–763, https://doi.org/10.4491/KSEE.2014.36.11.758.
[37] Y. Sakai, C.M. Nielsen, Y. Sato, S. Kato, Y. Kansha, Evaluation of the dependence of microbial fuel cells on soil composition and water content, Chem. Eng. Trans. 94 (2022) 619–624, https://doi.org/10.3303/CET2294103.
[38] M. Mejía-López, O. Lastres, J.L. Alemán-Ramírez, A. Verde, J.C. Alvarez, S. Torres-Arellano, G.N. Trejo-Díaz, P.J. Sebastian, L. Verea, Improvement of power density and COD removal in a sediment microbial fuel cell with α-FeOOH nanoparticles, Catalysts 14 (2024) 561, https://doi.org/10.3390/catal14090561.
[39] H.-U.-D. Nguyen, D.-T. Nguyen, K. Taguchi, A portable soil microbial fuel cell for sensing soil water content, Meas. Sens. 18 (2021) 100231, https://doi.org/10.1016/j.measen.2021.100231.